Effect of lithocholic acid on biologically active α,β-unsaturated aldehydes induced by H_2O_2 in glioma mitochondria for use in glioma treatment

DAN WANG[5*], LI BIE[1*], YANBIN SU[2,3], HAORAN XU[2], FENGRONG ZHANG[4], YANWEN SU[3] and BO ZHANG[1]

[1]Department of Neurosurgery, First Hospital of Jilin University; [2]Key Laboratory for Molecular Enzymology and Engineering, Jilin University, Changchun, Jilin 130021; [3]College of Chemical and Pharmaceutical Engineering, Jilin Institute of Chemical Technology, Changchun, Jilin 132022; [4]Jilin Institute for Food and Drug Control, Changchun, Jilin 130033; [5]Department of Ophthalmology, First Hospital of Jilin University, Changchun, Jilin 130021, P.R. China

Received January 8, 2017; Accepted February 21, 2018

DOI: 10.3892/ijmm.2018.3530

Abstract. Lithocholic acid (LCA) is known to kill glioma cells while sparing normal neuronal cells. However, the anti-glioma mechanism of LCA is unclear at present. Although malondialdehyde (MDA) is not specific to detect tumors, biologically active α,β-unsaturated aldehydes can be used to detect the outcome of gliomas, especially the mitochondria, as a research tool. The purpose of this research was to determine the optimum conditions for a lipid peroxidation model, according to changes in the aldehydes formed from the reaction between 2-thiobarbituric acid and biologically active α,β-unsaturated aldehydes. Experimental methods and procedures were successfully established for a model of lipid peroxidation induced by H_2O_2 in glioma mitochondria for glioma treatment and optimum conditions for LCA treatment were determined. The optimal conditions for the model were a glioma mitochondrial concentration of 1.5 mg/ml, H_2O_2 concentration of 0.3 mg/ml, duration of action of 30 min, and addition of 4.0 ml of 46 mM thiobarbituric acid. The effect of LCA, as determined by changes in the UV peaks at 450, 495, and 532 nm, was optimal at a concentration of 100 μM, a duration of action of 15 min, and in an acidic microenvironment. The study concluded that a suitable concentration of LCA has anti-glioma effects as determined by the effect on changes in the UV peaks at 450, 495 and 532 nm and the mitochondrial model developed should be conducive to further in-depth research.

Correspondence to: Dr Bo Zhang, Department of Neurosurgery, First Hospital of Jilin University, 71 Xinmin Street, Changchun, Jilin 130021 P.R. China
E-mail: zhangbo_366@hotmail.com

*Contributed equally

Key words: lithocholic acid, lipid peroxidation, aldehydes, H_2O_2, mitochondria

Introduction

Lithocholic acid (LCA) has been observed to kill rat glioma cells, which implies that it has an antitumor effect via mitochondrial outer membrane permeabilization (MOMP) (1). However, the exact anti-glioma mechanism of LCA is at present unclear. MOMP brings about the release of cytochrome c from the mitochondrial intermembrane space into the cytosol (2-4), which indicates that MOMP is closely related to the function of the mitochondrial inner membrane. The presence of reactive oxygen species (ROS) can lead to severe damage to cellular structures and their functions followed by cell death. Proton leak, likely induced by lipid peroxidation, and backed into the matrix of the mitochondria (5), and limited production of ROS (6) results in the uncoupling of oxidative phosphorylation. Uncoupling is brought about via the leak of protons through downstream lipid peroxidation products other than ATP synthase (7,8). Lipid peroxidation by ROS causes free radical reactions resulting in various aldehyde products, including trans-4-hydroxynonenal (4-HNE). 4-HNE is a toxic by-product of free radical damage (9) and is also a cell mediator acting as a signaling molecule. Lipid peroxidation products and ROS are very active in DNA binding and usually cause mutations that trigger oncogenesis (10).

The thiobarbituric acid (TBA) test was used to assay lipid peroxidation (11), but with other studies were different, focused on the effects of LCA on glioma mitochondria. H_2O_2 was chosen as the inducer of lipid peroxidation in this model and changes in UV peaks caused by reactions between TBA and biologically active α,β-unsaturated aldehydes (12) were used as indicators of reaction. The effects of LCA on UV peaks was investigated using a model of lipid peroxidation in mitochondria induced by H_2O_2. Changes in UV peaks corresponded to a variety of aldehydes as follows. 4-HNE (13), a major peak at 530 nm and shoulder peaks at 495 and 450 nm; trans, trans-muconaldehyde (14), a major peak at 495 nm and shoulder peaks at 460 and 530 nm; trans, trans-2,4-nonadienal, which is a dehydration product of 4-HNE, a major peak at 532 nm and shoulder peaks at 450 and 495 nm; acrolein (15), a major peak at 495 nm and shoulder peaks at 460 and 530 nm; crotonaldehyde (16), a major peak at

495 nm and shoulder peaks at 460 and 530 nm; malondialdehyde (MDA) (17), a major peak at 532 nm and a shoulder peak at 495 nm; no peaks from propionaldehyde (18) were observed under any experimental conditions.

Although MDA is not a specific indicator to detect tumors, the presence of biologically active α,β-unsaturated aldehydes (19) can be used to detect glioma, especially in mitochondria. In the present study, mitochondria were used to evaluate the correlation between LCA and observed changes in the UV spectrum at 495, 532 and 450 nm. The purpose of the study was to explore the anti-glioma mechanism of LCA on mitochondria.

Materials and methods

Materials. The reagents potassium chloride (KCl), 4-(2-hydroxyethyl)-1-piperazineethanesulfonic acid (HEPES), magnesium chloride hexahydrate ($MgCl_2$), ethylene diamine tetraacetic acid (EDTA), albumin from bovine serum (BSA), sodium chloride (NaCl), ferrous chloride ($FeCl_2$), 2-thiobarbituric acid (TBA), glacial acetic acid,1,1,3,3-tetramethoxypropane, trichloroacetic acid (TCA), butylated hydroxytoluene (BHT) were all of analytical grade; 30% hydrogen peroxide (H_2O_2) and lithocholic acid were obtained from Aladdin Industrial Corporation, Shanghai, China. Glioma mitochondria were obtained from glioma (Department of Neurosurgery, First Hospital of Jilin University). Mitochondrial extraction was performed on a Beckman Coulter Avanti J-26XPI. UV detection was performed on a 2550 UV-visible spectrophotometer (Beckman Coulter, Tokyo, Japan) and a PharmaSpec UV-1700 UV-Visible spectrophotometer (Shimadzu Corp., Tokyo, Japan). The pH detection used a PB-10pH/ATC electrode (Sartorius, Göttingen, Germany). Samples were treated with a 3K15 desktop high-speed refrigerated centrifuge (Sigma, Steinheim, Germany). Cold isolation medium consisted of 120 mM KCl, 20 mM HEPES (pH 7.4), 2 mM $MgCl_2$, 1 mM EGTA, 5 mg/ml BSA, prepared in advance, and cooled at 4˚C.

Reagent setup. The 50 mM NaCl and 0.2 mM $FeCl_2$ reagent was freshly prepared by dissolving 730 mg NaCl and 9.94 mg $FeCl_2$ in 250 ml distilled water. The reagent must be prepared fresh before use on the day, stored in a cool and dark place, and used within 4 h.

The LCA reagent was prepared by dissolving 19.41 mg 97% LCA in 50 ml heated ethanol and measuring 0, 50, 100, 150, 200 and 300 μl aliquots of 1 mM LCA and bringing to a final volume of 2 ml with distilled water, resulting in 0, 25, 50, 75, 100 and 150 μM solutions, respectively.

The 7.5% (W/V) TCA solution was prepared by weighing 7.50 g TCA in 100 ml distilled water.

The 46 mM TBA reagent was freshly prepared by dissolving 1.3464 g TBA in 200 ml 99% glacial acetic acid, then adding 6 ml of 2% butylated hydroxytoluene. The resulting solution was kept in the dark.

The 2% butylated hydroxytoluene solution was prepared by dissolving 120 mg of 99% butylated hydroxytoluene in 6 ml of 99% ethanol with heating.

Preparation of glioma mitochondria. With the approval of Institute Ethics Committee and the informed consent signed by the glioma patients or their guardians, the glioma samples were collected. Mitochondria derived from glioma were prepared by a modification of the conventional method of differential centrifugation (20). Briefly, 3.00 g of glioma tissue in fresh was immediately excised and minced in 150 ml ice cold isolation medium containing 120 mM KCl, 20 mM HEPES, pH 7.4, 2 mM $MgCl_2$, 1 mM EDTA and 5 mg/ml BSA. Minced blood-free tissue was rinsed and suspended in the same fresh medium and stirred. The sample was carefully homogenized with a tightly fitted homogenizer: 10,000 revolutions, 10 sec each time, interval of 15 sec, glioma tissue homogenate three times. After homogenization, isolation medium was added to the homogenate and centrifuged at 600 x g for 10 min. The resulting pellets were removed and the supernatant suspension was again centrifuged at 17,000 x g for 10 min. The supernatant was decanted and the pellets were gently resuspended in isolation medium and then centrifuged at 7,000 x g for 10 min. The supernatant was discarded and the precipitated pellets were resuspended in isolation medium, centrifuged at 3,500 x g for 10 min, and the supernatant containing the mitochondrial fraction was collected. All mitochondrial isolation procedures were performed at 0-4˚C. The concentration of the mitochondrial protein was estimated using Lowry's method (21) using BSA as the standard (50 mg protein/ml). The mitochondrial suspensions were used within 4 h.

The establishment of a model using UV peak changes to investigate aldehydes formed from lipid peroxidation induced by H_2O_2 in glioma mitochondria. A model relating to changes in UV peaks from aldehydes after lipid peroxidation induced by H_2O_2 in mitochondria was established using the following procedures. To samples containing 2 ml 50 mM NaCl and 0.2 mM $FeCl_2$ was added 0, 0.5, 1.0, 1.5, 2.0 and 2.5 mg/ml of glioma mitochondria and 1.76, 8.80, 17.60, 26.40, 35.20 and 70.40 μM of H_2O_2, respectively. Samples of mitochondrial lipid peroxidation at 1, 5, 10, 20, 30 and 40 min were prepared for extraction of aldehydes. Extracted samples (2 ml) were added to 4.3 ml of 7.5% (W/V) TCA, mixed and centrifuged at 5,000 x g for 10 min, then kept at 36˚C in a bath for 10 min, centrifuged again at 5000 x g for 10 min and another 4.3 ml of 7.5% (W/V) TCA was added. The aldehyde extract of lipid peroxidation in mitochondria was filtered using 12.50 mm medium speed filter paper for determination. The reaction of the aldehydes in lipid peroxidation with TBA and the formed adducts were determined with spectrophotometric methods (12). The procedure was performed as described by Ottino and Duncan (22) with some modifications. The 2 ml sample extract and 1.0, 1.5, 2.0, 2.5, 3.0 and 4.0 ml of TBA reagent were mixed in 4 ml test tubes and heated in a boiling water bath for 15 min. The reaction mixture was chilled and centrifuged at 5,000 x g for 10 min. The absorbance of samples over the wavelength range 400-600 nm was measured using a 2550 UV-visible spectrophotometer, focused on changes in absorbance at 450, 495 and 532 nm using distilled water as a blank, adjustable light transmittance of 100%.

Determination of factors effecting the impact of LCA on the reaction of aldehydes in lipid peroxidation in glioma mitochondria. The effect of LCA on the reaction of aldehydes in lipid peroxidation in glioma mitochondria was investigated at

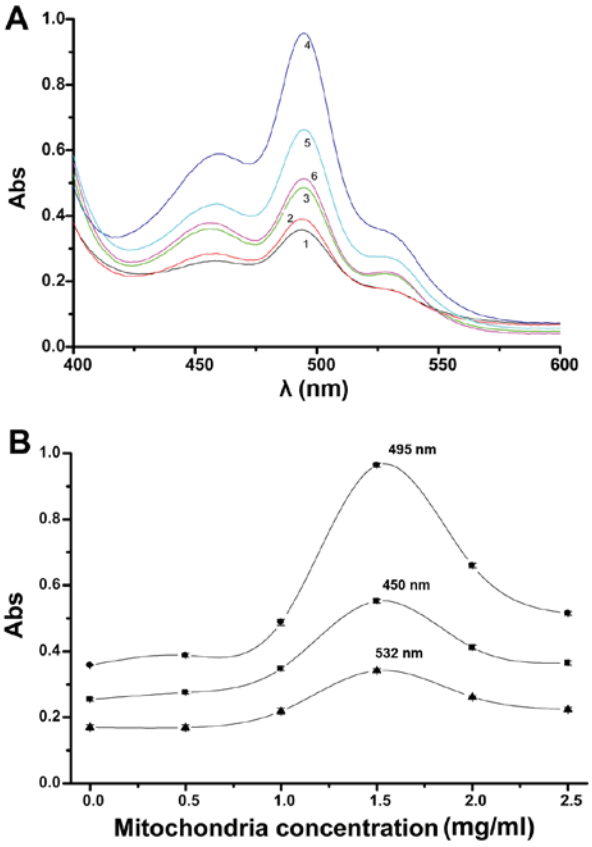

Figure 1. Impact of mitochondrial concentrations deriving from glioma on UV peak changes from aldehydes in the lipid peroxidation model (A). 1, 2, 3, 4, 5 and 6 indicate 0, 0.5, 1.0, 1.5, 2.0 and 2.5 mg/ml concentrations of glioma mitochondria, respectively [20 min, 17.60 μM H_2O_2, 4.0 ml thiobarbituric acid (TBA)]. The absorbance curves at 495, 450 and 532 nm with changing concentrations of the glioma mitochondria were observed separately (B).

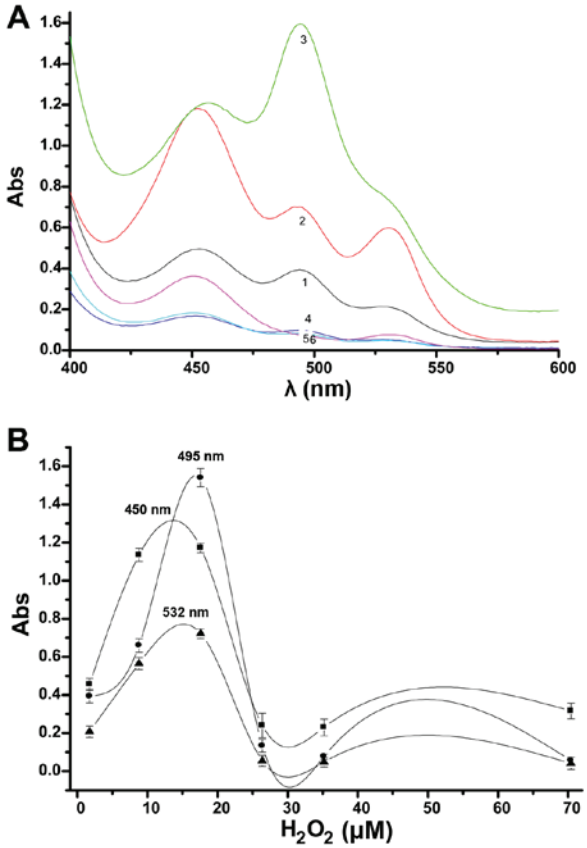

Figure 2. Effect of H_2O_2 on UV peak changes from aldehydes in the lipid peroxidation model (A). 1, 2, 3, 4, 5 and 6 indicate 1.76, 8.80, 17.60, 26.40, 35.20 and 70.40 μM concentrations of H_2O_2, respectively [20 min, 1.5 mg/ml mitochondria, 4.0 ml thiobarbituric acid (TBA)]. The absorbance changes at 495, 450 and 532 nm with H_2O_2 concentrations are shown (B).

different LCA concentrations (0, 25, 50, 75, 100 and 150 μM), reaction times (0, 5, 10, 15, 20 and 30 min), and micro environmental pH (3.0, 7.0, 8.0).

Statistical treatment. Statistic software Origin 8.0 was used to perform one-way analysis of variance for the experimental data.

Results

UV peaks change in the spectra of aldehydes in lipid peroxidation induced by H_2O_2 in glioma mitochondria. The influence of different mitochondrial concentrations on UV peak changes from aldehydes in the lipid peroxidation model is shown in Fig. 1A. Increasing concentrations of glioma mitochondria showed a commensurate rise in lipid peroxidation. When the mitochondrial concentrations were >1.50 mg/ml, a trend towards a decrease in lipid peroxidation was observed. There are three peaks that can be observed with a change in mitochondrial concentration; a major peak at 495 nm and two shoulder peaks at 532 and 450 nm. The 532 nm peak is much weaker than the 450 nm peak. All three peaks changed in a concentration-dependent manner, this was seen especially in the main peak at 495 nm. When the mitochondrial concentration was 1.5 mg/ml, all three peaks changed noticeably.

The absorbance curves at 495, 450 and 532 nm with changing concentrations of the glioma mitochondria are shown in Fig. 1B. The 450 and 532 nm curves were similar in shape, the change in the 450 nm peak was greater than the change at 532 nm. The change in the curve at 495 nm, especially at a mitochondrial concentration of 1.5 mg/ml, was much more pronounced than in the other two curves. The results indicate that at a glioma mitochondrial concentration of 1.5 mg/ml, the absorbances at 495, 450 and 532 nm were sensitive, prominent, and significant, particularly the peak change at 495 nm.

The effect of H_2O_2 concentrations on the UV peaks from aldehydes in the lipid peroxidation model are shown in Fig 2A. When concentrations were higher than 17.60 μM, the three peaks decreased substantially, this is especially reflected in the peaks at 495 and 532 nm. At low concentrations, the three peaks show an obvious change. In the low concentration range with increasing concentrations, the peak at 495 nm gradually became larger, as did the peak at 450 nm to a lesser extent, and the peak of 532 nm showed the least change. Results indicated that a concentration of 17.60 μM H_2O_2 leads to three substantial changes in UV peaks, but the appearance of the peak of 532 nm was not as obvious. While at a concentration of 8.8 μM H_2O_2, the size of the three peaks was substantially decreased, but three distinct peaks were observed; therefore, this concentration is more appropriate for use in the glioma mitochondrial lipid peroxidation model. When 8.80 μM is selected as the experimental concentration, the model shows that the major peak at 450 nm changes the

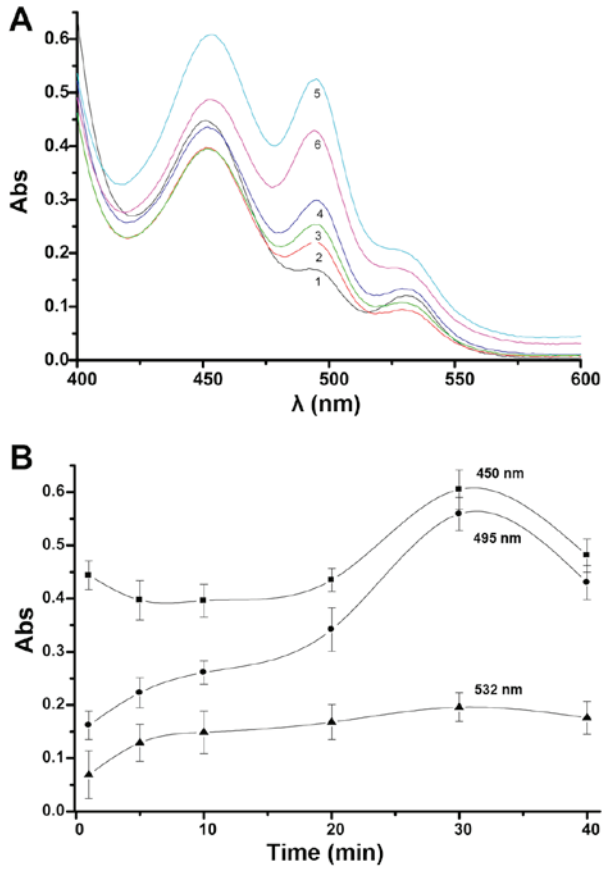

Figure 3. Time influence of H_2O_2 on mitochondria with regard to UV peak changes from aldehydes in the lipid peroxidation model (A). 1, 2, 3, 4, 5 and 6 indicate after 1, 5, 10, 20, 30 and 40 min, respectively (8.8 μM H_2O_2, 1.5 mg/ml mitochondria, 4.0 ml TBA). The absorbance curves at peaks of 495, 450 and 532 nm with changing of time were observed (B).

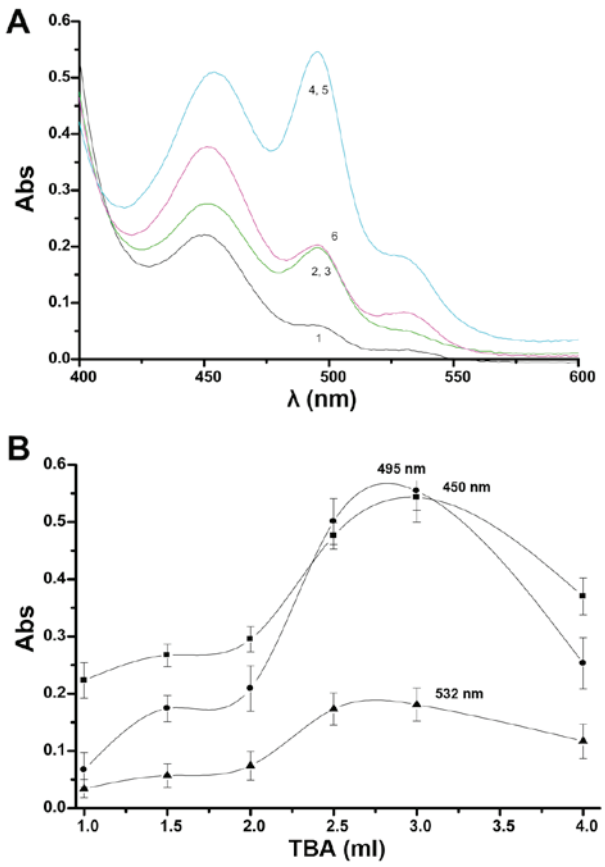

Figure 4. The optimum amount of thiobarbituric acid (TBA) for reaction with the extracted aldehydes. Changes in the UV peaks from aldehydes in the lipid peroxidation model (A). 1, 2, 3, 4, 5 and 6 indicate 1.0, 1.5, 2.0, 2.5, 3.0 and 4.0 ml TBA reagent, respectively. The absorbance peaks at 495, 450 and 532 nm with changing amount of TBA are shown (B).

most, followed by the peak at 495 nm, and the peak at 532 nm is relatively weak.

Changes in absorbance were accompanied by changes in H_2O_2 concentration, as shown in Fig. 2B. When the H_2O_2 concentration is low, the three peaks were sensitive to changes in the concentration of H_2O_2. The change in the 495 nm peak was the most pronounced; changes in the 450 nm peak were similar to the 532 nm peak, with a greater change observed at 450 nm. Therefore, the peak at 495 nm is the most important indicator to observe apoptosis induction of glioma cells.

The effects over time of H_2O_2 on glioma mitochondria with regard to changes in the UV peaks from aldehydes in the lipid peroxidation model can be seen in Fig. 3A. After H_2O_2 was added to the mitochondrial suspension, the establishment of lipid peroxidation in glioma mitochondria required an appropriate time. The experimental results show that three distinct peaks are apparent, a major peak at 450 nm, a large shoulder peak at 495 nm and a smaller shoulder peak at 532 nm. At different times, graphs of the three peaks appear similar in shape. When the reaction time is 30 min, the three peaks changed the most noticeably, over this time, the peak change became small. In this case, detection of absorbance at 450 and 495 nm was a sensitive indicator of the effects.

In the initial few minutes after H_2O_2 addition to glioma mitochondria, there are some differences in the three absorbance curves, and after 30 min the curves at 450 and 495 nm displayed obvious changes, while the curve at 532 nm was only gradually slightly elevated. After 30 min, the absorbance of the three peaks showed a downward trend, as seen in Fig. 3B.

The selection of the optimum amount of TBA for the reaction with the extracted aldehydes to assess the UV peak changes from aldehydes in the lipid peroxidation model is shown in Fig. 4A. When the amount of TBA increased, three peaks gradually appeared in the UV spectra, first a peak at 450 nm, then 495 nm and finally at 532 nm. When the amount of TBA was low, the three peaks appeared gradually in order, but with low absorbance. When the amount of TBA reached 2.5 ml, the three peaks appeared at the maximum absorbance value and when the amount of TBA was further increased, the peaks tended to become smaller with decreased amplitude. The changes in the three peaks were significant, stable, and sensitive with amounts of TBA from 2.5 to 3.0 ml, but when the amount of TBA reached 2.5 ml, the 532 nm peak was not obvious. All three peaks decreased substantially when the amount of TBA was 4.0 ml.

Changes in the peaks with differing amounts of TBA can be seen in Fig. 4B. No curves changed greatly when the amount of TBA was 2.0 ml or less. Further increases in the amount of TBA resulted in curves with prominent and sensitive characteristics. The curves reached a maximum when the amount of TBA was 3.0 ml, the peaks were especially high at 495 and 450 nm. Above 3.0 ml TBA, each curve declines, but the decline in the 532 peak was not as obvious. Therefore, detection would be most effective when using 4.0 ml TBA.

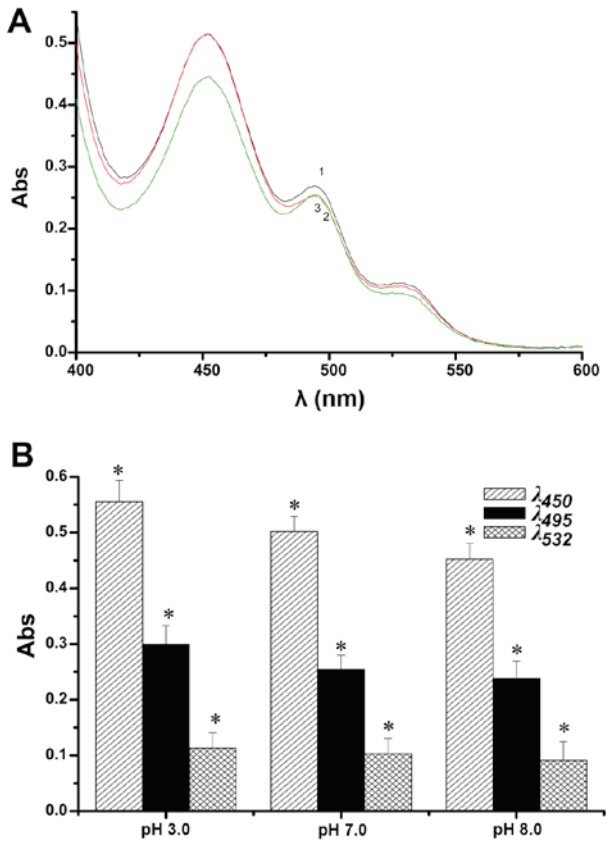

Figure 5. Contribution of pH related to lithocholic bile acid on changes in UV peaks from aldehydes in the lipid peroxidation model (A). 1, 2 and 3 indicate pH 3.0, 7.4 and 8.0, respectively. The absorbance changes at 495, 450 and 532 nm peaks with pH changes were observed separately (B). Compared with the normal control group, statistically significant difference, *p<0.05.

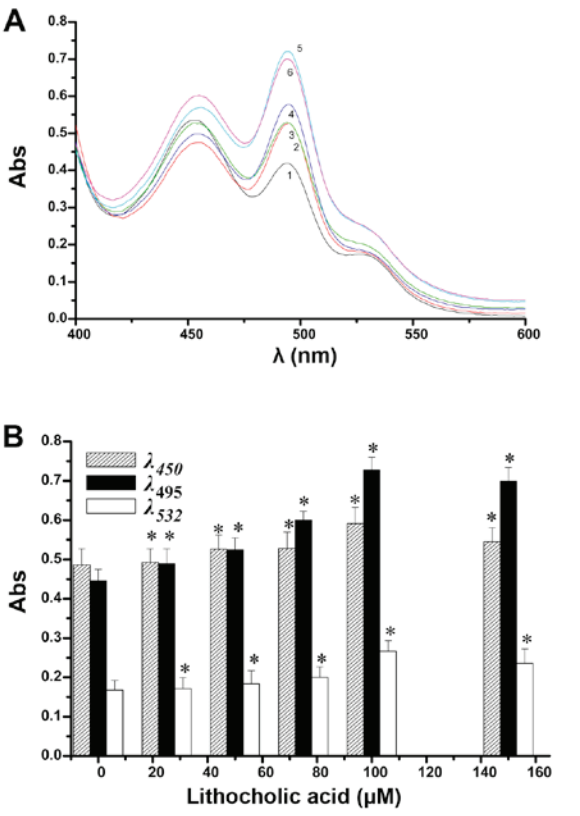

Figure 6. Effect of lithocholic acid concentrations on changes in UV peaks from aldehydes in the lipid peroxidation model (A). 1, 2, 3, 4, 5 and 6 indicate 0, 25, 50, 75, 100 and 150 μM lithocholic acid (LCA), respectively. The absorbance peaks at 495, 450 and 532 nm with changing concentrations of lithocholic acid are shown (B). Compared with the normal control group, statistically significant difference, *p<0.05. (20 min, pH 7.4).

In conclusion, the conditions established for the glioma mitochondrial lipid peroxidation model were a concentration of glioma mitochondria of 1.5 mg/ml, H_2O_2 concentration of 8.80 μM, a time of 30 min for the reaction of H_2O_2 with glioma mitochondria, and an amount of 46 mM TBA for optimum reaction with the extracted aldehydes of 4.0 ml. The indices for evaluation in the model were the peak changes at 495, 450 and 532 nm.

Using the above-mentioned conditions for the lipid peroxidation model, the contribution of pH on the changes in the UV peaks from aldehydes in the lipid peroxidation model are displayed in Fig. 5A. In addition to the main peak at 450 nm, there was a large shoulder peak at 495 nm and a smaller shoulder peak at 532 nm. The absorbance of the three peaks at different pH microenvironments is shown in Fig. 5B. With a decrease in pH, the three peaks gradually increased, in particular the peaks at 450 and 495 nm. The results indicate that the three peaks in acidic and alkaline microenvironments are quite prominent, especially in the former. In short, an acidic microenvironment greatly promoted cell apoptosis.

Effect of LCA on changes in aldehyde concentration after lipid peroxidation in glioma mitochondria. Using the above mentioned conditions for the lipid peroxidation model, the effect of LCA concentrations on changes in the UV peaks from aldehydes was investigated and the results are given in Fig. 6A. Under conditions of ≤100 μM LCA, increases in LCA increased the peaks at 495, 450 and 532 nm, in a concentration-dependent manner, especially the peak at 495 nm. A concentration of >100 μM, led to the peak at 495 nm decreasing, as seen in Fig. 6B. These results show that in the model of mitochondrial lipid peroxidation via measuring an increase in aldehydes, addition of LCA caused further rapid peroxide production to achieve an anti-glioma effect. The LCA antitumor contribution is reflected in the changes in the peak at 495 nm, followed by the peak at 450 nm and with less contribution from the peak at 532 nm. As determined from the peaks from the different aldehydes, LCA increased the amounts of 4-HNE, trans, trans-muconaldehyde, trans, trans-2,4-nonadienal, acrolein, crotonaldehyde and MDA to produce an antitumor effect.

The effects over time of LCA addition on the change in the UV peaks from aldehydes in the lipid peroxidation model can be seen in Fig. 7A. At ≤30 min, LCA elicits three UV absorption peaks, at 495, 450 and 532 nm. The main peak was at 495 nm, followed by a large shoulder peak at 450 nm and a small shoulder peak at 532 nm. The intensity of the three peaks first increased with increasing time and then decreased. As shown in Fig. 7B, after ≤15 min and with time of operation of LCA prolonged, the peaks changed significantly, especially the peaks at 495 and 450 nm. After >15 min, a downward trend in the peaks can be clearly observed. The results show that when the reaction time of LCA was 15 min, the three peaks displayed the most sensitive and pronounced change, particularly the peaks at 495 and 450 nm, while the change in the peak at 532 nm showed relatively poor sensitivity.

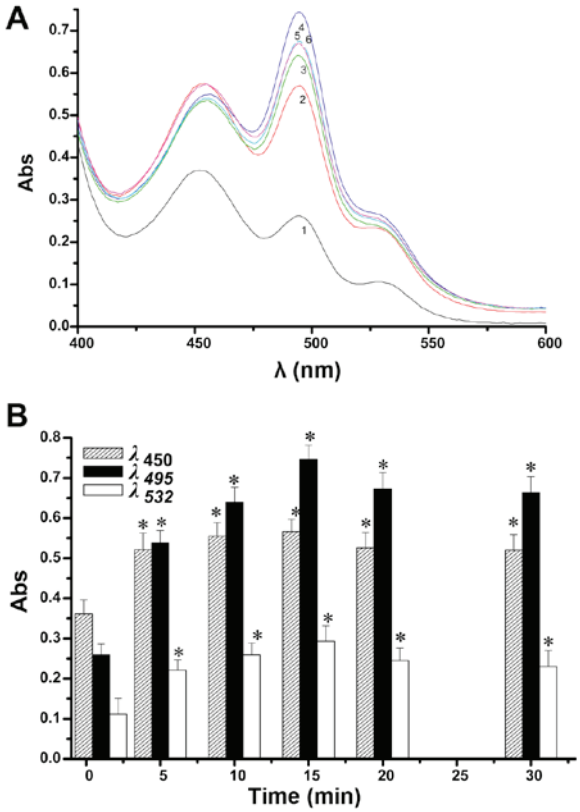

Figure 7. The effects over time of lithocholic acid (LCA) addition on the change in the UV peaks from aldehydes in the lipid peroxidation model (A). 1, 2, 3, 4, 5 and 6 indicate 0, 5, 10, 15, 20 and 30 min reaction times, respectively. The absorbance changing curves at 495, 450 and 532 nm with changing reaction times were observed separately (B). Compared with the normal control group, statistically significant difference, *p<0.05. (150 μM LCA, pH 7.4).

Discussion

LCA is a kind of bile acid. Recently, low concentrations of LCA have been shown to make BE(2)-m17 and SK-n-MCIXC cells sensitive to H_2O_2-induced death of apoptotic cells, which was regulated by mitochondria. Certain concentrations could make primary cultures of human neurons resistant to death. In the treatment of glioma, research into efficient, hypotoxic drugs which can induce glioma cell apoptosis is of current importance. While the antitumor effect of LCA is just corresponding to it. However, the molecular biological mechanisms of the antitumor effect of LCA is not clear at present. Therefore, research into the antitumor mechanisms of LCA is of great importance to the research and development of anti-glioma drugs. In a recent study, the oxygen radical has been determined to be the most important radical affecting the body (23). Besides direct damage to the body, the oxygen radical mostly can make the cells, especially the polyunsaturated fatty acids of mitochondrial membrane peroxide, to damage the cytomembrane, as well as affecting the structure and function of the mitochondrial membrane. These effects could lead to energy metabolism disturbance causing damage to the cell functions (24). Lipid peroxidation can generate unsaturated aldehydes, which are the signaling molecules of the mitochondria. Lipid peroxidation may also activate cell apoptosis pathways, such as Fas/FasL, to induce cell apoptosis (25). Biologically active α,β-unsaturated aldehydes can be used to detect effects on glioma after development of an appropriate glioma mitochondria model.

A glioma mitochondrial lipid peroxidation model has been successfully established, in which three small peaks from aldehydes appear in the UV spectra after reaction with TBA. This model enables the exploration of the LCA anti-glioma mechanism. Small molecule aldehydes generated in the lipid oxidation process are closely linked to tumorigenesis, development and outcome. Such small molecule aldehydes can lead to the demise of glioma tissues and may have an important research value. After reaction with TBA, these small molecule aldehydes show three characteristic UV absorption peaks at 495, 450 and 532 nm (18). These results are in accordance with our study and indicate that small molecule aldehydes are the major reaction products in the lipid peroxidation model in glioma mitochondria.

The basis of the glioma mitochondrial model is cell death as a consequence of lipid peroxidation. H_2O_2 generated in an aerobic environment leads to toxic levels of DNA damage (26-29). Cells are more damaged when exposed to H_2O_2 in low concentrations for a long time than for a short time. The mechanism of cell death caused by H_2O_2 is through regulation of iron in the mitochondrial inner membrane because cell-permeable iron chelators effectively prevent H_2O_2-mediated DNA damage in cells (30-32). The role of small molecule aldehydes, such as 4-HNE, in H_2O_2-induced cell death remains to be elucidated.

4-HNE, the most cytotoxic aldehyde (13), is generated in lipid peroxidation by degradation of omega-3-polyunsaturated fatty acids (33). 4-HNE along with other small molecule aldehydes possesses the capacity to block cell proliferation and lead to cell death in <60 min (9). In addition, DNA polymerase, a thiol enzyme (34), was blocked by the sulfhydryl reactive agents, HNE and acrolein (35). HNE-GSH adducts display a feedback inhibition on GSH transferases. Unlike ROS, which have been associated with cell proliferation and differentiation (36,37), aldehydes in lipid peroxidation linger a comparatively long time and can diffuse from the initial site to reach distant targets. These kinds of small molecule aldehydes react with nucleic acids, contributing to mutagenesis and carcinogenesis (38). Aldehydes are detected based on the formation of aldehydes in lipid peroxidation. The basic process leading to the production of aldehydes is via the β-cleavage reaction of lipid hydroperoxides, more accurately described as lipid alkoxy-radicals (33). 4-HNE and its dehydration product trans, trans-nonadienal react with TBA to form chromogens absorbed maximally at 530 and 532 nm. Other biologically active α,β-unsaturated aldehydes, including E-2-butenal, acrolein, crotonaldehyde, trans-muconaldehyde also react with TBA, absorbing maximally at 495 nm (18). These characteristic absorption peaks appear to provide a strong support for the detection of biologically active α,β-unsaturated aldehydes.

These aldehydes bind stably with thiols under acidic conditions, leading to the condensation of the small molecule aldehydes, and participation in the death of glioma (33,39). Of course, glutathione easily reacts in a neutral environment with α,β-unsaturated aldehydes (40). The reaction of α,β-unsaturated aldehydes with thiols in an environment of pH ≥7.0 can proceed up to hundred times faster than in an acidic environment, which explains the results observed with LCA in an acidic environment. A concentration of <0.1 μM

HNE may be regarded as a normal physiological level, but at a range of 0.1-20 μM, HNE may attack target thiol proteins and inhibit DNA and protein synthesis within the lipid bilayer (34). In addition, the effects accompanying cell death in the process of lipid peroxidation include the rapid depletion of glutathione (41), a decrease in protein thiols (42), inhibition of DNA, RNA and protein synthesis (43), and morphological changes. Therefore, the reaction of α,β-unsaturated aldehydes with the thiols in proteins has important significance (44).

The reaction of MDA with nucleosides has been shown to be promoted by an acidic environment and acrolein, which was the strongest electrophile and showed the highest reactivity with thiols can be formed during lipid peroxidation (45).

Acrolein, which is highly cytotoxic to cells, reacted approximately over a hundred times faster with GSH than crotonal or HNE (40). The mechanism of the reaction of acrolein and crotonal with GSH is basically the same as HNE. When acrolein causes rapid depletion of thiols, the thiols in proteins become progressively modified (46) and then acrolein-treated DNA does not act as substrate for DNA-methylase (47). Crotonal has much lower toxicity than acrolein. MDA, a low molecular aldehyde is produced from ROS attacking polyunsaturated fatty acids.

In conclusion, the optimum conditions for a lipid peroxidation model using glioma mitochondria have been investigated according to changes in UV peaks at 495, 450 and 532 nm after reaction between TBA and biologically active α,β-unsaturated aldehydes. The optimal conditions determined for the lipid peroxidation model in glioma mitochondria were a mitochondrial concentration of 1.5 mg/ml, H_2O_2 concentration of 0.3 mg/ml, a duration of action of 30 min, and addition of 4.0 ml of 46 mM TBA. The model indicators were changes in the peaks at 495, 450 and 532 nm related to aldehydes formed during lipid peroxidation of glioma mitochondria induced by H_2O_2. The effect of LCA on the peaks at 450, 495 and 532 nm was greatest when the conditions were an LCA concentration of 100 μM, a duration of action of 15 min, and an acidic microenvironment, according to the mitochondria model. The mechanism of LCA anti-glioma action may be interpreted as regulation and control of the aldehydes represented by changes in peaks at 450, 495 and 532 nm, and the use of the glioma mitochondrial model may be conducive to in-depth research in this topic.

In conclusion, the impact of LCA on glioma was closely related to the production of aldehydes from lipid peroxidation in the glioma mitochondria. The optimum conditions have been confirmed according to changes in the peaks at 495, 450 and 532 nm using a lipid peroxidation model in glioma mitochondria, by means of reactions between TBA and biologically active α,β-unsaturated aldehydes. Mitochondrial modeling in glioma lipid peroxidation was successfully established and the optimal conditions were determined to be a glioma mitochondrial concentration of 1.5 mg/ml, a H_2O_2 concentration of 0.3 mg/ml, a duration of action of 30 min, and addition of 4.0 ml of 46 mM TBA. The model indicators were changes in the peaks at 495, 450 and 532 nm related to aldehydes formed during lipid peroxidation of glioma mitochondria induced by H_2O_2. The effect of LCA on the peaks at 450, 495 and 532 nm was greatest when the conditions were an LCA concentration of 100 μM, a duration of action of 15 min and an acidic microenvironment according to the newly created mitochondria model. LCA caused increases in peaks at 450, 495 and 532 nm. These three peaks, especially the peak at 495 nm, represent the formation of α,β-unsaturated aldehydes, which could induce glioma cell apoptosis by several pathways. We believe that LCA may induce glioma cell apoptosis by increasing the concentration of α,β-unsaturated aldehydes from lipid peroxidation production in glioma mitochondria. In addition, the glioma mitochondrial model will be conducive to further in-depth research.

Acknowledgements

The authors would like to express their gratitude to all those who helped them during the experiment. Their deepest gratitude goes first and foremost to Professor Zhengqiang Li who is the leader of Key Laboratory for Molecular Enzymology and Engineering, Jilin University. He supported the authors with equipments and technical guidance through all the stages of the experiment. Without his consistent and selfless support, this experiment could not be finished successfully.

Funding

This study was supported by the development plan project of Jilin Province Science and Technology, China (no. 20120946), the doctoral fund project, Jilin Institute of Chemical Technology, China (no. 2012121), the National Natural Science Foundation of China (no. 81201980), the Natural Science Foundation of Jilin Province, China (nos. 20130522028JH and 20130101149JC) and the Youth Science Foundation of First Hospital of Jilin University, China (no. JDYY72016010).

Availability of data and material

All data generated or analyzed during this study are included in this published article.

Authors' contributions

YanbinS analyzed and interpreted the experiment data. BZ designed the study, collected the samples and interpreted the data. DW and LB were involved in drafting the manuscript and revising it critically for important intellectual content. YanwenS and HX performed the UV detection. FZ was a major contributor in specimen processing and mitochondrial collection. All authors read and approved the final manuscript.

Ethics approval and consent to participate

The drug clinical trial and research was approved by the Ethics Committee of the First Hospital of Jilin University (2012)Trial NO(2012-105).

Consent for publication

Not applicable.

Competing interests

The authors declare that they have no competing interests.

References

1. Goldberg AA, Beach A, Davies GF, Harkness TA, Leblanc A and Titorenko VI: Lithocholic bile acid selectively kills neuroblastoma cells, while sparing normal neuronal cells. Oncotarget 2: 761-782, 2011.
2. Tait SW and Green DR: Mitochondria and cell death: Outer membrane permeabilization and beyond. Nat Rev Mol Cell Biol 11: 621-632, 2010.
3. Jourdain A and Martinou JC: Mitochondrial outer-membrane permeabilization and remodelling in apoptosis. Int J Biochem Cell Biol 41: 1884-1889, 2009.
4. Parsons MJ and Green DR: Mitochondria in cell death. Essays Biochem 47: 99-114, 2010.
5. Miwa S and Brand MD: Mitochondrial matrix reactive oxygen species production is very sensitive to mild uncoupling. Biochem Soc Trans 31: 1300-1301, 2003.
6. Parker N, Vidal-Puig A and Brand MD: Stimulation of mitochondrial proton conductance by hydroxynonenal requires a high membrane potential. Biosci Rep 28: 83-88, 2008.
7. Papa S and Skulachev V: Reactive oxygen species, mitochondria, apoptosis and aging. In: Detection of Mitochondrial Diseases. Gellerich FN and Zierz S (eds). Springer, p305-319, 1997.
8. Brand MD: Uncoupling to survive? The role of mitochondrial inefficiency in ageing. Exp Gerontol 35: 811-820, 2000.
9. Esterbauer H, Schaur RJ and Zollner H: Chemistry and biochemistry of 4-hydroxynonenal, malonaldehyde and related aldehydes. Free Radic Biol Med 11: 81-128, 1991.
10. Lee YS and Wurster RD: Potentiation of anti-proliferative effect of nitroprusside by ascorbate in human brain tumor cells. Cancer Lett 78: 19-23, 1994.
11. Halliwell B and Chirico S: Lipid peroxidation: Its mechanism, measurement, and significance. Am J Clin Nutr 57 (Suppl 5): 715S-725S, 1993.
12. Draper HH and Hadley M: Malondialdehyde determination as index of lipid peroxidation. Methods Enzymol 186: 421-431, 1990.
13. Benedetti A, Comporti M and Esterbauer H: Identification of 4-hydroxynonenal as a cytotoxic product originating from the peroxidation of liver microsomal lipids. Biochim Biophys Acta 620: 281-296, 1980.
14. Witz G, Rao GS and Goldstein BD: Short-term toxicity of trans, trans-muconaldehyde. Toxicol Appl Pharmacol 80: 511-516, 1985.
15. Patton S and ParkKurtz GW: A note on the thiobarbituric acid test for milk lipid oxidation. J Dairy Sci 38: 901, 1955.
16. Esterbauer H, Cheeseman KH, Dianzani MU, Poli G and Slater TF: Separation and characterization of the aldehydic products of lipid peroxidation stimulated by ADP-$Fe2^{+}$ in rat liver microsomes. Biochem J 208: 129-140, 1982.
17. Sinnhuber RO, Yu TC and Yu TC: Characterization of the red pigment formed in the 2-thiobarbituric acid determination of oxidative rancidity. J Food Sci 23: 626-634, 1958.
18. Witz G, Lawrie NJ, Zaccaria A, Ferran HE Jr and Goldstein BD: The reaction of 2-thiobarbituric acid with biologically active alpha,beta-unsaturated aldehydes. J Free Radic Biol Med 2: 33-39, 1986.
19. Inci S, Özcan OE and Kilinç K: Time-level relationship for lipid peroxidation and the protective effect of α-tocopherol in experimental mild and severe brain injury. Neurosurgery 43: 330-335, discussion 335-336, 1998.
20. Nulton-Persson AC and Szweda LI: Modulation of mitochondrial function by hydrogen peroxide. J Biol Chem 276: 23357-23361, 2001.
21. Lowry OH, Rosebrough NJ, Farr AL and Randall RJ: Protein measurement with the Folin phenol reagent. J Biol Chem 193: 265-275, 1951.
22. Ottino P and Duncan JR: Effect of alpha-tocopherol succinate on free radical and lipid peroxidation levels in BL6 melanoma cells. Free Radic Biol Med 22: 1145-1151, 1997.
23. Malecki EA: Manganese toxicity is associated with mitochondrial dysfunction and DNA fragmentation in rat primary striatal neurons. Brain Res Bull 55: 225-228, 2001.
24. Hartley A, Stone JM, Heron C, Cooper JM and Schapira AH: Complex I inhibitors induce dose-dependent apoptosis in PC12 cells: Relevance to Parkinson's disease. J Neurochem 63: 1987-1990, 1994.
25. Sugiyama A and Sun J: Immunochemical detection of lipid hydroperoxide-and aldehyde-modified proteins in diseases. In: Lipid Hydroperoxide-Derived Modification of Biomolecules. Kato Y (ed). Springer. pp115-125, 2014.
26. Park S, You X and Imlay JA: Substantial DNA damage from submicromolar intracellular hydrogen peroxide detected in Hpx- mutants of *Escherichia coli*. Proc Natl Acad Sci USA 102: 9317-9322, 2005.
27. Demple B, Halbrook J and Linn S: *Escherichia coli* xth mutants are hypersensitive to hydrogen peroxide. J Bacteriol 153: 1079-1082, 1983.
28. Carlsson J and Carpenter VS: The $recA^{+}$ gene product is more important than catalase and superoxide dismutase in protecting *Escherichia coli* against hydrogen peroxide toxicity. J Bacteriol 142: 319-321, 1980.
29. Imlay JA and Linn S: Bimodal pattern of killing of DNA-repair-defective or anoxically grown *Escherichia coli* by hydrogen peroxide. J Bacteriol 166: 519-527, 1986.
30. Imlay JA, Chin SM and Linn S: Toxic DNA damage by hydrogen peroxide through the Fenton reaction in vivo and in vitro. Science 240: 640-642, 1988.
31. Mello Filho AC, Hoffmann ME and Meneghini R: Cell killing and DNA damage by hydrogen peroxide are mediated by intracellular iron. Biochem J 218: 273-275, 1984.
32. Bar-Or D and Winkler JV: Copper is involved in hydrogen-peroxide-induced DNA damage. Free Radic Biol Med 32: 197-199, 2002.
33. Van Kuijk FJ, Holte LL and Dratz EA: 4-Hydroxyhexenal: A lipid peroxidation product derived from oxidized docosahexaenoic acid. Biochim Biophys Acta 1043: 116-118, 1990.
34. Petersen DR and Doorn JA: Reactions of 4-hydroxynonenal with proteins and cellular targets. Free Radic Biol Med 37: 937-945, 2004.
35. Wawra E, Zollner H, Schaur RJ, Tillian HM and Schauenstein E: The inhibitory effect of 4-hydroxy-nonenal on DNA-polymerases alpha and beta from rat liver and rapidly dividing Yoshida ascites hepatoma. Cell Biochem Funct 4: 31-36, 1986.
36. Goldkorn T, Balaban N, Matsukuma K, Chea V, Gould R, Last J, Chan C and Chavez C: EGF-Receptor phosphorylation and signaling are targeted by H_2O_2 redox stress. Am J Respir Cell Mol Biol 19: 786-798, 1998.
37. Huang RP, Peng A, Golard A, Hossain MZ, Huang R, Liu YG and Boynton AL: Hydrogen peroxide promotes transformation of rat liver non-neoplastic epithelial cells through activation of epidermal growth factor receptor. Mol Carcinog 30: 209-217, 2001.
38. Petruzzelli S, Hietanen E, Bartsch H, Camus AM, Mussi A, Angeletti CA, Saracci R and Giuntini C: Pulmonary lipid peroxidation in cigarette smokers and lung cancer patients. Chest 98: 930-935, 1990.
39. Esterbauer H and Zollner H: Methods for determination of aldehydic lipid peroxidation products. Free Radic Biol Med 7: 197-203, 1989.
40. Esterbauer H, Zollner H and Scholz N: Reaction of glutathione with conjugated carbonyls. Z Naturforsch C 30: 466-473, 1975.
41. Poot M, Verkerk A, Koster JF, Esterbauer H and Jongkind JF: Influence of cumene hydroperoxide and 4-hydroxynonenal on the glutathione metabolism during in vitro ageing of human skin fibroblasts. Eur J Biochem 162: 287-291, 1987.
42. Dogterom P, Mulder GJ and Nagelkerke JF: Lipid peroxidation-dependent and -independent protein thiol modifications in isolated rat hepatocytes: Differential effects of vitamin E and disulfiram. Chem Biol Interact 71: 291-306, 1989.
43. Poot M, Verkerk A, Koster JF, Esterbauer H and Jongkind JF: Reversible inhibition of DNA and protein synthesis by cumene hydroperoxide and 4-hydroxy-nonenal. Mech Ageing Dev 43: 1-9, 1988.
44. Esterbauer H: Kinetics of the reaction of sulfhydryl compounds with alpha-beta-unsaturated aldehydes in aqueous system. Monatsh Chem 101: 782-810, 1970.
45. Witz G: Biological interactions of α,β-unsaturated aldehydes. Free Radic Biol Med 7: 333-349, 1989.
46. Grafström RC, Dypbukt JM, Willey JC, Sundqvist K, Edman C, Atzori L and Harris CC: Pathobiological effects of acrolein in cultured human bronchial epithelial cells. Cancer Res 48: 1717-1721, 1988.
47. Cox R, Goorha S and Irving CC: Inhibition of DNA methylase activity by acrolein. Carcinogenesis 9: 463-465, 1988.